Direct synthesis of hydrogen peroxide using Cs-containing heteropolyacid-supported palladium-copper catalysts.

Faisal Alotaibi[a], Sulaiman Al-Mayman[a], Mohammad Alotaibi[a], Jennifer K. Edwards[b], Richard J. Lewis[b], Raja Alotaibi[a], Graham J. Hutchings[b]

[a] National Center for Petrochemicals Technology, King Abdulaziz City for Science and Technology, P.O. Box 6086, Riyadh 11442, Kingdom of Saudi Arabia
[b] Cardiff Catalysis Institute, School of Chemistry, Cardiff University, Main Building, Park Place, Cardiff CF10 3AT, UK

ABSTRACT

The direct synthesis of hydrogen peroxide (H_2O_2) from molecular hydrogen and oxygen could represent a green and economically attractive alternative to the current indirect anthraquinone process used for the industrial production of hydrogen peroxide. This reaction has been investigated using palladium supported on the Cs-containing heteropolyacid $Cs_{2.5}H_{0.5}PW_{12}O_{40}$. In addition, the effect of adding copper as a potential activity promoter was investigated. These catalysts were also evaluated for the subsequent degradation of hydrogen peroxide. The catalytic activity of the 0.5 wt.%Pd/$Cs_{2.5}H_{0.5}PW_{12}O_{40}$ catalyst towards hydrogen peroxide synthesis was greater than that of both the mono-metallic Cu or bi-metallic Pd-Cu analogues with the incorporation of Cu to Pd resulting in a significant decrease in catalytic selectivity for the formation of hydrogen peroxide. Moreover, 0.5 wt.%Pd/$Cs_{2.5}H_{0.5}PW_{12}O_{40}$ also showed low activity towards the degradation of hydrogen peroxide. Hence the use of the Cs-containing heteropolyacid as a support for Pd gives higher rates of hydrogen peroxide formation when compared with different supported Pd catalysts prepared using supports used in previous studies.

KEY WORDS: Green Chemistry; Copper; Palladium; Bimetallic catalysts; Heteropolyacids; Hydrogen peroxide.

INTRODUCTION

Hydrogen peroxide (H_2O_2), a green oxidant, is widely used in the chemical industry and environmental protection. Currently H_2O_2 is primarily used as a bleaching agent in the pulp and paper industry [1-3], as a disinfectant in the cosmetic and pharmaceutical industry, as an oxidant in water treatment [4, 5] and in the synthesis of bulk chemicals [6]. It is also used, in a highly purified form, for etching and cleaning in the electronics' industry [7]. The increasing demand for H_2O_2 has in part been driven for growing global demand for propene oxide, which finds application in the production of surfactants, polyurethane and resins [8]. It is estimated that by 2020 global annual demand for H_2O_2 will reach 5.2 million tons [9].

Current production of H_2O_2 on an industrial scale is limited to the well-established anthraquinone process, which is based on the process developed by Riedl and Pfleiderer of BASF in 1939 [10]. Although highly efficient, there are significant costs around the need for

continual replacement of the H_2 carrier molecule, which undergoes unselective hydrogenation and the need to use stabilizing agents, in particular acids, to prevent the decomposition of H_2O_2 while in transit. With the presence of these acids often leading to reactor corrosion and increased costs associated with their downstream removal.

The direct synthesis of H_2O_2 from molecular H_2 and O_2 is an attractive means for producing H_2O_2 at point of use, overcoming many of the economic and environmental drawbacks associated with the anthraquinone process. However, catalytic selectivity towards H_2O_2 production has long been an issue surrounding the direct synthesis approach. With many catalysts often requiring the use of halide [11-12] or acid additives [13] to minimize the over hydrogenation or decomposition pathways, which result in the unselective production of H_2O, as shown in Figure 1.

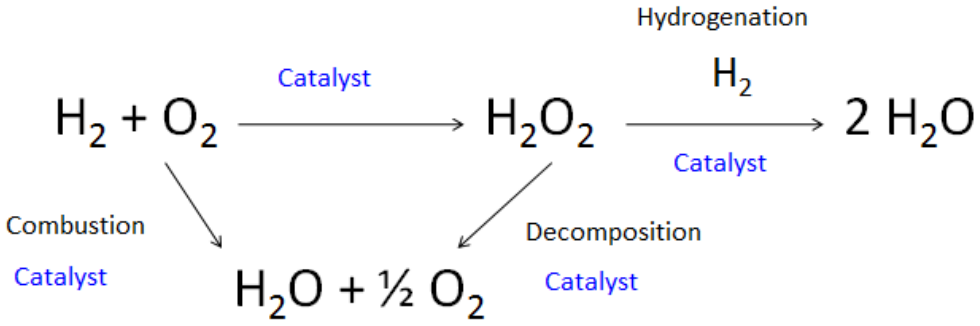

Figure 1. The reaction pathways involved in the direct synthesis of H_2O_2 reaction

Bimetallic AuPd catalysts have been shown to be significantly more selective towards H_2O_2 generation compared to analogous Pd supported catalysts, likely due to a combination of ensemble and electronic effects. Since the initial report of the activity of Au towards the direct synthesis of H_2O_2 by Landon et al.[14] the effect of Au addition to Pd-based catalysts has been well established in the literature on a range of common supports [15, 16]. With subsequent work investigating the combination of Pd with other precious metals including Pd-Pt [17, 18], Pd-Ru [19], Pd-Ir [20] and Pd-Ag [21, 22]. Deguchi et al. have recently compared the effect of the addition of precious metals to a Pd-polyvinylpyrrolidone colloid, with significant enhancements in catalytic activity observed with the addition of very low (0.5 at.%) concentrations of Pt and Ir [20]. However, the replacement of Au with a cheaper, more abundant, base metal would clearly be beneficial from an economic standpoint. We have recently reported that it is possible to significantly enhance the selectivity of Pd-based catalysts towards H_2O_2 through the encapsulation of small Pd nanoparticles in a suitable secondary metal oxide, removing the requirement of Au incorporation to achieve a highly selective Pd catalyst in the absence of acid or halide stabilizing agents [23]. With subsequent studies further demonstrating the remarkable effects of Pd modification by Sn [24, 25]. While others have investigated the beneficial effects of Zn [26], Ni [27], and Te [28] into Pd nanoparticles, with computational studies by Xu et al. predicting Pd-Pd and Pd-W as potential candidates for highly active catalysts for the direct synthesis of H_2O_2 [29].

It is well known that the choice of support can dramatically effect catalytic selectivity towards H_2O_2, with those more acidic supports beneficial for catalytic selectivity and net yield of H_2O_2 [30]. Due to their high acidity numerous studies have investigated the use of heteropolyacids

as both catalyst supports [31, 32] as well as solid acid additives used in addition to well established catalysts [33]. However, issues of low surface area and high solubility in polar solvents have dictated the need for the introduction of specific cations such as Cs^+, K^+ and Rb^+ into the structure of the heteropolyacid or immobilization onto mesoporous supports [34, 35] Park et al.[31, 32, 36, 37] and Sun et al. [38] have previously investigated the use of monometallic Pd nanoparticles supported on insoluble heteropolyacid (HPA) catalysts for the direct synthesis of H_2O_2 in the absence of any acid and/or halide additives. Sun et al. [38] have reported that Pd nanoparticles supported on HPAs comprising the Keggin structure showed higher H_2O_2 productivities with a corresponding improvement in H_2O_2 selectivity compared to conventional monometallic-Pd catalysts supported on common oxides. While, Park et al. [32] have investigated the effect of varying the extent of Cs-incorporation into the Keggin structure of Pd-exchanged heteropolyacids ($Pd_{0.15}Cs_xH_{2.7-x}PW_{12}O_{40}$) for H_2O_2 synthesis and report that catalytic activity is correlated with support acidity. Building on this work we investigated the effect of Au addition to these systems by both impregnation and ion-exchange, which resulted in an increased rate of H_2O_2 synthesis compared to the monometallic Pd catalysts, again demonstrating the beneficial effect of Au incorporation into a Pd catalyst [39, 40]. Indeed these catalyst show remarkable activity towards H_2O_2 synthesis under reaction conditions considered detrimental towards H_2O_2 [39]. More recently, we have demonstrated the dramatic enhancements in catalytic activity can be achieved when using insoluble Cs-exchanged phosphotungstic acid as a heterogeneous additive alongside a standard H_2O_2 synthesizing catalyst, with a near three-fold improvement in H_2O_2 synthesis rate reported [33].

In this work, we extend these earlier studies and evaluate the performance of mono- and bi-metallic Pd and Cu catalysts supported on Cs-containing heteropolyacids and magnesium oxide for their activity towards the direct synthesis of H_2O_2.

EXPERIMENTAL SECTION

Preparation of $Cs_{2.5}H_{0.5}PW_{12}O_{40}$

The acidic salt $Cs_{2.5}H_{0.5}PW_{12}O_{40}$ (designated CsPW) were prepared by the addition of the required amount of aqueous cesium carbonate (0.47 M) drop-wise to an aqueous solution of $H_3PW_{12}O_{40}$ (0.75 M) at 40 ^{o}C with stirring. The obtained precipitate was aged in aqueous mixture for 48 h at room temperature and dried using a rotary evaporator at 45 ^{o}C/25 Torr.

Preparation of Cu-Pd /$Cs_{2.5}H_{0.5}PW_{12}O_{40}$

Monometallic Pd catalysts supported on $Cs_{2.5}H_{0.5}PW_{12}O_{40}$, (designated Pd/CsPW,) were synthesized by stirring the pre-formed CsPW support with the required amount of palladium (II) acetylacetonate solution, to achieve a nominal loading of 0.5 wt.%, together in toluene at room temperature for 1 h. This was followed by slow evaporation of toluene in a rotary evaporator. Following this, the resulting solid underwent thermal reduction (H_2, 250 ^{o}C, 2 h, 10 ^{o}Cmin^{-1}). The actual Cu and Pd content in the catalyst were determined by ICP. Monometallic Cu and bi-metallic Pd-Cu catalysts (designated Cu /CsPW and PdCu/CsPW) were synthesised using the same procedure with appropriate amounts of copper (II) acetylacetonate and palladium (II) acetylacetonate solutions to achieve the desired metal loadings. All catalysts were ground prior to calcination (150 °C/0.5 Torr, 1.5 h, 10 ^{o}Cmin^{-1})

Preparation of Cu-Pd /MgO

Monometallic Pd catalysts supported on MgO (designated Pd/MgO), were synthesised by stirring MgO powder (Lehmann) with required amount of palladium (II) acetylacetonate, to achieve a nominal loading of 0.5 wt.%. in toluene at room temperature for 1 h, followed by slow evaporation of toluene in a rotary evaporator. Following this, the resulting solid underwent thermal reduction (H_2, 250 ^{o}C, 2 h, ramp rate 10 ^{o}Cmin^{-1}). The actual copper and palladium contents in the catalyst were determined by ICP. Monometallic Cu and bi-metallic Pd-Cu supported catalysts (designated Cu / MgO and PdCu/ MgO respectively) were synthesised using the same procedure with appropriate amounts of copper (II) acetylacetonate and palladium (II) acetylacetonate to achieve the desired metal loading. All catalysts were ground prior to calcination (150 ^{o}C/ 0.5 Torr, 1.5 h, ramp rate 10 ^{o}Cmin^{-1}).

Catalyst characterization.

The phase identification and crystallinity of the prepared catalysts was identified using powder X-ray diffraction (XRD) on a Bruker X-ray diffractometer system equipped with a RINT 200 wide-angle goniometer using Ni-filtered Cu Kα radiation with a generator voltage and current of 40 kV and 30 mA, respectively. A scan speed of 5^{o} (2θ min^{-1}) with a scan step of 0.002^{o} (2θ) was applied during a continuous run in the 5-60^{o} (2θ) range. Phase identification was carried out using the reference database (JCPDS-files) supplied with the equipment.

Copper and palladium contents in the different catalysts were measured by inductively coupled plasma-optical emission spectrometry (ICP-OES) analysis (Agilent, ICP-700). The Brunauer-Emmett-Teller (BET) method, using a Quantachrome Corporation Autosorb, was used to determine the total surface area of the prepared catalysts by N_2 adsorption/desorption at -196 °C. FT-IR spectra were measured using a PerkinElmer Spectrum GX FT-IR spectrometer.

The catalyst morphology, structure, and elemental composition of the samples were analyzed with transmission electron microscopy (TEM) technique. TEM analysis was carried out by using the TitanG2 80-300 ST microscope from FEI Company (Hillsboro, OR) that was also equipped with energy dispersive spectrometer (EDS) from EDAX (Mahwah, NJ). Prior to the analysis, the TEM specimens were prepared by dispersing the powders in ethanol and then dropping the resulting suspension onto 400-mesh holey carbon-coated copper (Cu) grids. TEM-analysis include the bright-field TEM (BF-TEM) and high-angle-annular-dark-field scanning TEM (HAADF-STEM) techniques in conjunction with EDS to determine the above-mentioned properties of the prepared samples.

Samples were analysed using a Quantachrome instruments ChemBET TPD/R/O. The samples (0.02-0.05 g) were degassed at 110 ^{o}C for 1 h under helium to clean the surface prior to ammonia adsorption. The degassed sample was treated in a pure ammonia flow for 0.5 h at 60 ^{o}C before further heat treatment at 100 ^{o}C for 1 h to remove the physisorbed ammonia. The sample was then heated under helium to 800 ^{o}C at 20 ^{o}C min^{-1} and the ammonia desorption monitored by TCD.

Catalyst Testing.

Direct Synthesis of H_2O_2.

Catalyst testing was performed using Parr Instruments stainless steel autoclave batch reactor (equipped with an overhead stirrer and temperature/pressure sensors) with a nominal volume of 70 ml and a maximum working pressure of 14 MPa. To evaluate catalytic activity towards the direct synthesis of H_2O_2, the autoclave was charged with catalyst (0.01 g) and solvent (5.6 g MeOH and 2.9 g H_2O). The charged autoclave was purged three times with 5 %H_2/CO_2 (100 psi) and then filled with 5 %H_2/CO_2 (420 psi) and 25 %O_2/CO_2 (160 psi). The temperature was allowed to decrease to 2 ^oC followed by stirring (1200 rpm) of the reaction mixture for 0.5 h. H_2O_2 yield was determined by titrating aliquots of the final filtered solution with acidified $Ce(SO_4)_2$ (1.18×10^{-2} $molL^{-1}$). The $Ce(SO_4)_2$ solution was standardised against $(NH_4)_2Fe(SO_4)_2.6H_2O$ using ferroin as indicator.

H_2O_2 Degradation.

The reaction was carried out in the same stainless steel autoclave reactor described previously. Before charging the autoclave with the catalyst and solvent mixture, the initial moles of H_2O_2 were determined by titrating aliquots of the initial solvent mixture (0.68 g H_2O_2 (50wt.%) 2.22 g H_2O and 5.6 g MeOH) with acidified $Ce(SO_4)_2$ (1.18×10^{-2} mol L^{-1}). The autoclave was then charged with the catalyst (0.01 g), solvent (0.68 g H_2O_2, 2.22g H_2O and 5.6 g MeOH), purged three times with 5 %H_2/CO_2 (100 psi) and then filled with 5 %H_2/CO_2 (420 psi). The temperature was allowed to decrease to 2 ^oC followed by stirring (1200 rpm) of the reaction mixture for 0.5 h. The final concentration of H_2O_2 was determined by titration of aliquots of the final filtered solution with acidified $Ce(SO_4)_2$ (1.18×10^{-2} mol L^{-1}). The $Ce(SO_4)_2$ solution was standardised against $(NH_4)_2Fe(SO_4)_26H_2O$ using ferroin as indicator. The hydrogenation of H_2O_2 was determined by the following calculation:

$$\text{Moles of } H_2O_2 \text{ consumed} = \text{Mol } H_2O_{2\ \text{INIAL}} - \text{Moles } H_2O_{2\ \text{FINAL}}$$

$$\text{Degradation} = \left(\text{Moles of } H_2O_2 \text{ consumed} / \text{kg}_{\text{cat}} \times \text{h}\right)$$

Results and discussion.

Catalyst Characterization.

XRD analysis of the three $Cs_{2.5}H_{0.5}PW_{12}O_{40}$ based catalysts; CsPW, 0.5 wt.%Cu/CsPW, and 0.5 wt.% Cu-0.5 wt.% Pd/CsPW, as seen in Figure 2, revealed no reflections associated with Cu and or Pd indicating the high dispersion of these species. Indeed regardless of the immobilisation of Pd and Cu the reflections observed can all be assigned to $Cs_{2.5}H_{0.5}PW_{12}O_{40}$, with negligible change in peak width, or intensity observed with Pd and Cu immobilisation, the detected reflections consistent with the cubic structure of $H_3PW_{12}O_{40}$ (ICDD reference number 00-050-0657).

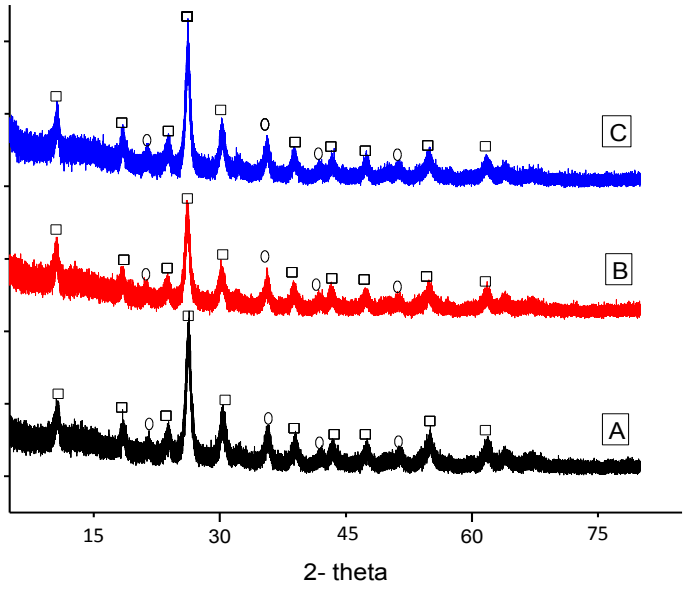

Figure 2: Powder XRD diffractograms of freshly prepared catalysts supported on CsPW. A: CsPW, B: 0.5wt.%Cu/CsPW, C: 0.5 wt.%Cu-0.5wt.%Pd/CsPW

Figure 3 shows the XRD patterns for the three MgO (which is used as an example of a basic oxide support) supported catalysts: 0.5 wt.%Cu/MgO, 0.5 wt.% Pd-0.5 wt.% Cu/MgO, and 0.5 wt.%Pd/MgO. It can be observed that the crystal structure of MgO (ICDD reference number 01-0178-0430) was maintained upon incorporation of Cu and Pd metals. Interestingly, unlike with the analogous CsPW supported catalyst, reflections associated with PdO can be observed for the monometallic 0.5 wt.%Pd /MgO catalyst, as seen in Figure 3, (2θ =39.8, 46.5, 67.93). However, upon addition of Cu these reflections are no longer observed, indicating the potential ability of Cu to better disperse Pd.

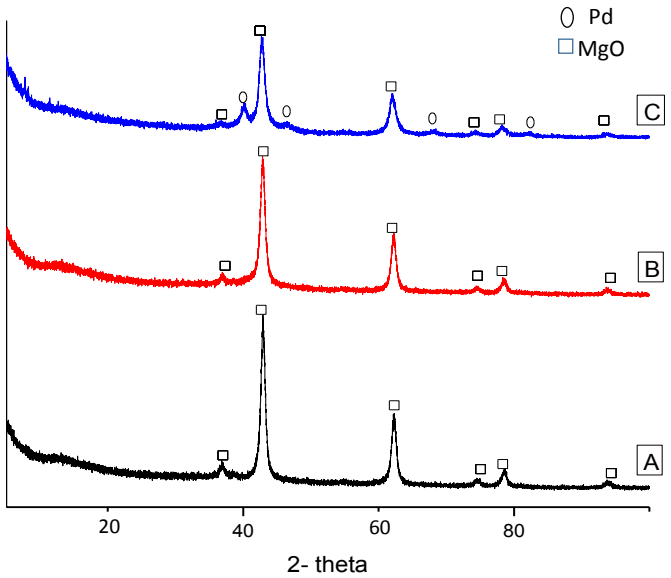

Figure 3: Powder XRD diffractograms of freshly prepared catalysts supported on MgO. A: 0.5wt.%Cu/MgO, B: 0.5wt.%Cu- 0.5 wt.%Pd/MgO, C: 0.5wt.%Pd/MgO

ICP analysis was used in order to determine the variation between theoretical and actual metal loadings with the results seen in Table 1. Reasonable agreement was obtained between the actual content and calculated content for each metal of Cu and Pd in all Cs-containing heteropolyacid-supported catalysts**.**

Table 1: Total metal loading of Cu and Pd supported catalysts as determined by ICP analysis.

	Cu / wt.%		Pd / wt.%	
Catalyst	Calc.	Actual	Calc.	Actual
0.5 wt.% Cu/CsPW	0.5	0.46	-	-
0.5 wt % Cu-0.5 wt.% Pd/CsPW	0.5	0.44	0.5	0.53
0.5 wt.% Pd/CsPW	-	-	0.5	0.48
0.5 wt.% Cu/MgO	0.5	0.45	-	-
0.5 wt.% Cu-0.5 wt.% Pd/MgO	0.5	0.46	0.5	0.47
0.5wt.% Pd/MgO	-	-	0.5	0.46

Surface area analysis of the catalysts was determined by N_2 adsorption and the results are given in Table 2. Park et al. [41] have previously reported that upon Cs-incorporation the surface area of the parent phosphotungstic acid increases significantly, from 6 m^2/g to 105 m^2/g which is in keeping with surface areas reported in Table 2.

Table 2. Surface area and pore analysis as determined via N_2 adsoption.

Catalyst	**Surface Area (m^2/g)**	**Pore size (A°)**	**Pore volume (cm^3/g)**
0.5 wt.% Cu/CsPW	109	0.110	0.43
0.5 wt.% Cu-0.5 wt.%Pd/CsPW	95	0.095	0.39
0.5 wt.% Pd/CsPW	105	0.101	0.37
0.5 wt.% Cu/MgO	145	48	0.85
0.5 wt.% Cu-0.5 wt.% Pd/MgO	136	42	0.78
0.5 wt.% Pd/MgO	152	47	0.80

FT-IR analysis of the 0.5 wt.%Cu/CsPW, 0.5 wt.%Pd/CsPW and 0.5 wt.%Cu-0.5 wt.%Pd/CsPW catalysts can be seen in Figure 4. It can be observed that the spectral positions of the peaks were similar for all compounds and showed the characteristic features of phosphotungstic acids comprising the Keggin structure have been maintained after metal loading, indicating that the bulk structure of the catalysts remain unchanged after metal immobilisation. Moreover, it can be observed that four peaks are mainly observed. These peaks have been assigned in previous study [42] with the first peak at 1080-1060 cm^{-1} corresponding to a v_{as} ($P\text{-}O_a$) vibration mode, the second peak at 990-960 cm^{-1} to a v_{as} ($W\text{-}O_d$) vibration mode,

the third peak at 900-870 cm^{-1} to a v_{as} (M-O_b-M) vibration mode and the fourth peak at 810-780 cm^{-1} to a v_{as} (M-O_c-M).

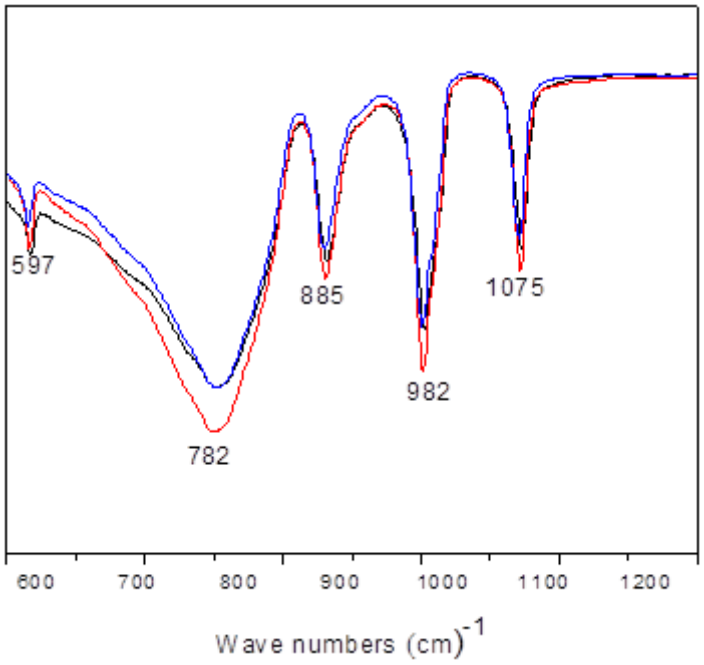

Figure 4: FT-IR spectra of the fresh prepared catalysts: Red: 0.5 wt.%Cu-0.5 wt.%Pd/CsPW, Blue: 0.5 wt.%Pd/CsPW, Black: 0.5 wt.%Cu /CsPW

Investigation of the 0.5 wt.%Cu/CsPW, 0.5 wt.%Cu- 0.5 wt.%Pd/CsPW and 0.5 wt.% Pd/CsPW and the analogous MgO supported catalysts by transmission electron microscopy (TEM) are shown in the Figure 5 and Figure 6 . For both supports, no distinct nanoparticles are observed, indicating that Pd and Cu are well dispersed on the MgO and CsPW supports.

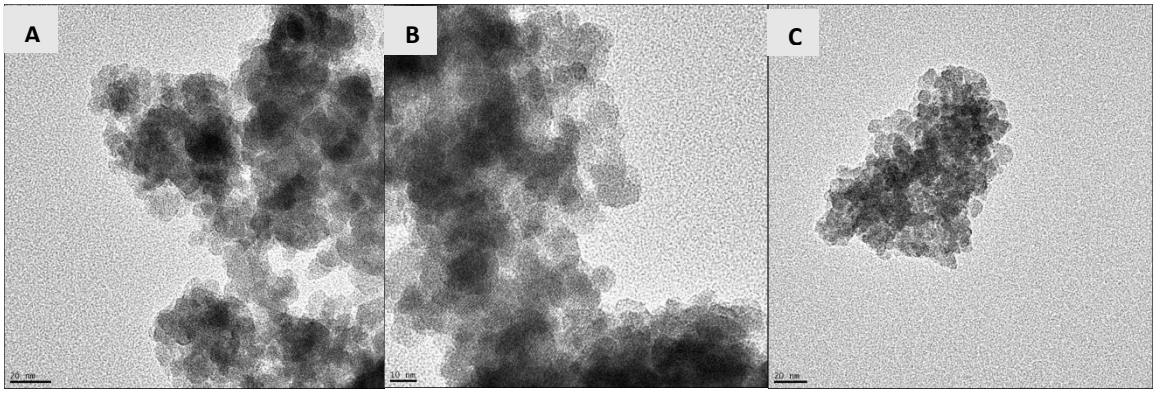

Figure 5: TEM micrographs of (a) 0.5wt.%Cu/CsPW, (b) 0.5wt.%Cu-0.5wt.%Pd/CsPW, (c) 0.5wt.%Pd/CsPW.

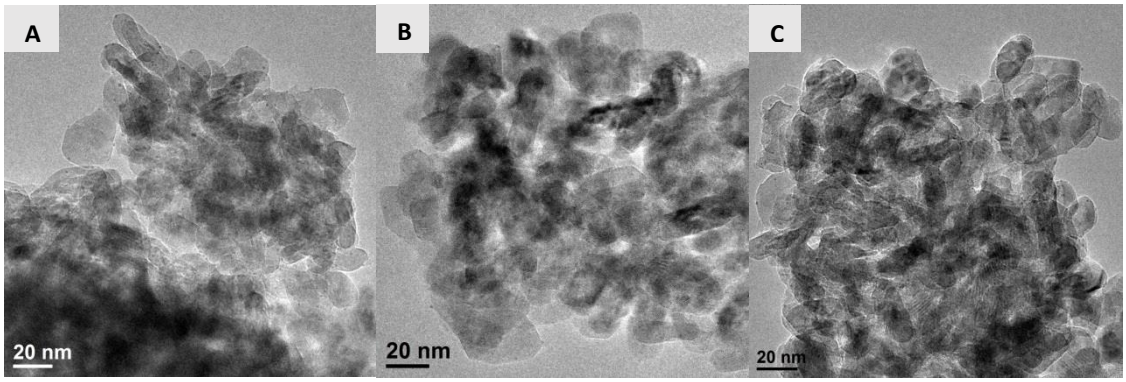

Figure 6: TEM micrographs of (a) 0.5%Cu/MgO, (b) 0.5%Cu-0.5%Pd/MgO, (c) 0.5%Pd/MgO.

NH_3-TPD analysis, as seen in Figure 7A-F, were carried out in order to elucidate the nature of the acid sites present for the Cs-exchanged tungstophosporic acid supported palladium and copper mono- and bi-metallic catalysts. Total acidity (NH_3 uptake) calculated from the peak area for all samples, and compared to the acidity of standard ZSM-5 material is summarized in Table 3. Pd/CsPW catalyst exhibited larger acidity than Cu/CsPW and Cu-Pd/CsPW. It can be seen that the bimetallic catalyst showed no acidity which might be attributed to the blockage of pores of CsPW by Cu-Pd clusters. The heteropolyacid supported catalysts were found to completely decompose at approximately 700 ^oC. The MgO supported samples displayed the largest NH_3 uptake and a complex desorption pattern compared to the heteropolyacid supported samples.

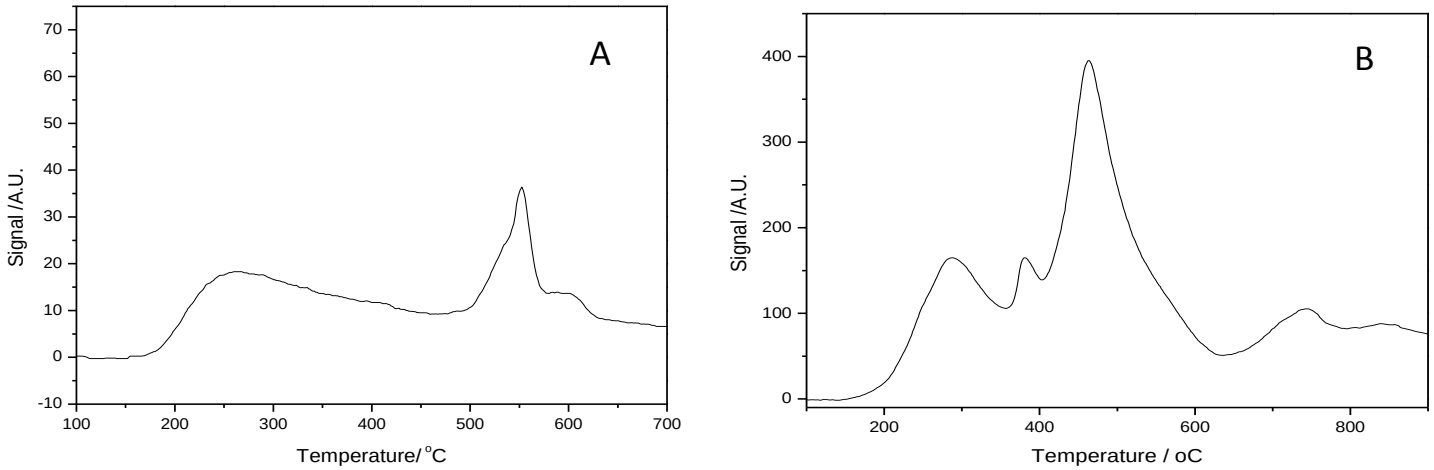

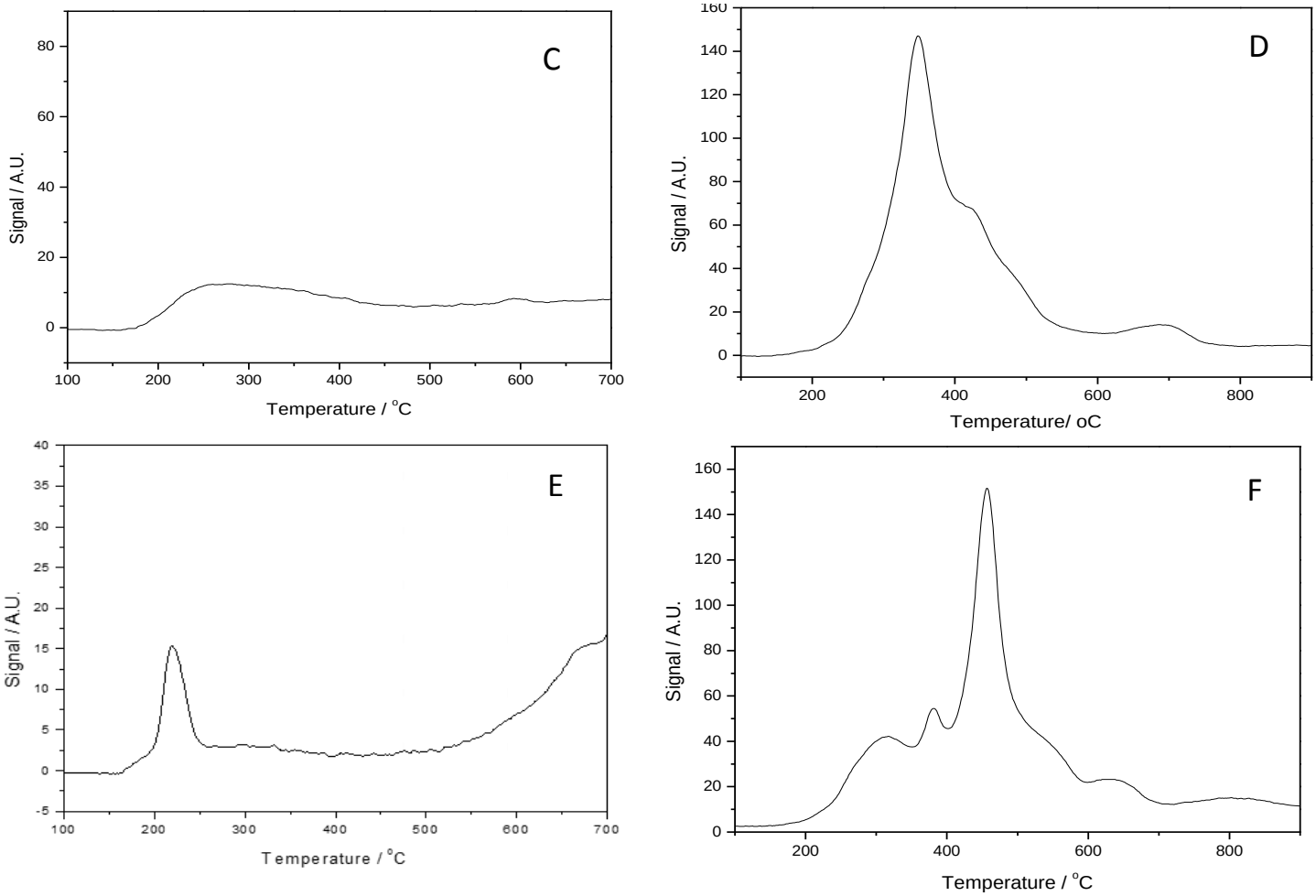

Figure 7: NH_3-TPD profiles of A: 0.5wt.%Cu/CsPW, B: 0.5wt.%Cu/MgO, C: 0.5wt.%Cu-0.5wt.%Pd/CsPW: D: 0.5wt.%Cu-0.5wt.%Pd/MgO; E: 0.5wt.%Pd/CsPW; F: 0.5wt.%Pd/MgO.

Table 3: Total acidity analysis using NH_3-TPD

Catalyst	NH_3 uptake/mmol/g
0.5 wt.% Cu/CsPW	0.08
0.5 wt.% Pd/CsPW	0.17
0.5 wt.% Cu-0.5 wt.% Pd/CsPW	0
0.5 wt.% Cu/MgO	9.29
0.5 wt.% Pd/MgO	6.48
0.5 wt.% Cu-0.5 wt.% Pd/MgO	6.97
ZSM-5	1.15

Catalytic performance towards the direct synthesis of hydrogen peroxide.

Table 4 shows the catalytic performance of the mono- and bi-metallic of Pd and Cu catalysts supported on Cs-containing heteropolyacids and MgO respectively for the direct synthesis of H_2O_2 as well as its subsequent degradation. The high activity of the 0.5 wt.% Pd/CsPW catalyst towards H_2O_2 synthesis should first be noted, despite a ten-fold decrease in Pd loading catalytic

activity is approximately 60 % of that reported for 5 wt.%Pd/$Cs_{2.8}H_{0.2}PW_{12}O_{40}$, possibly due to increased selectivity towards H_2O_2.

Comparison of the MgO and Cs-exchanged heteropolyacid support catalyst reveals the much greater selectivity of the CsPW supported catalyst, with the catalytic activity of the 0.5 wt.%Pd/CsPW and 0.5 wt.%Pd/MgO catalysts towards the degradation of H_2O_2 reported as 13 and 33 % respectively, and an associated increase in net yield of H_2O_2. This is in keeping with our previous work, investigating the role of support acidity in the direct synthesis of H_2O_2 [30] and confirms the ability of acidic supports to inhibit catalytic activity towards the degradation of H_2O_2 to H_2O.

Table 4: Catalytic activity of Pd and Cu monometallic and Cu-Pd bimetallic catalysts supported on Cs-containing heteropolyacids and magnesium oxide towards the direct synthesis and subsequent degradation of H_2O_2.

Catalyst	Productivity ($mol_{H2O2}kg_{cat}^{-1}h^{-1}$)[a]	H_2O_2 Degradation ($mol_{H2O2}kg_{cat}^{-1}h^{-1}$)[b]	Reference[c]
$Cs_{2.5}H_{0.5}PW_{12}O_{40}$	0	124	40
$Cs_{2.8}H_{0.2}PW_{12}O_{40}$	1	162	39
MgO	0	206	30
Pd based catalysts			
0.5 wt.% Pd/ CsPW	85	76	This study
$Pd_{0.15}Cs_{2.5}H_{0.2}PW_{12}O_{40}$	96	221	39
5 wt.%Pd/$Cs_{2.8}H_{0.2}PW_{12}O_{40}$	136	281	39
5 wt.% Pd/CeO_2	97	329	42
5 wt. % Pd /TiO_2	30	288	30
5 wt. % Pd /Al_2O_3	9	200	30
5 wt. % Pd /MgO	29	582	30
0.5wt.% Pd/ MgO	5	194	This study
Cu based catalysts			
0.5 wt.% Cu/ CsPW	0	0	This study
0.5wt.% Cu/ MgO	0	118	This study
Pd-Cu based catalysts			
0.5 wt.% Pd- 0.5 wt.% Cu / CsPW	4	41	This study
0.5 wt.% Pd- 0.5 wt.% Cu/MgO	0	118	This study

[a] Reaction conditions: Catalyst (0.01 g), 8.5 g solvent (2.9 g H_2O, 5.6 g MeOH), 5% H_2/CO_2 (420 psi), 25 % O_2/CO_2 (160 psi), 2 °C, 1200 rpm, 0.5 h. [b] Reaction conditions: Catalyst (0.01 g), H_2O_2 (0.68 g 50 wt.%), solvent (2.22 g H_2O, 5.6g MeOH), 5% H_2/CO_2 (420 psi), 2°C, 1200 rpm, 0.5 h. [c] Comparison of productivities for selected catalysts reported in the literature.

It can be seen that the H_2O_2 synthesis activtiy of the 0.5 wt.%Pd/CsPW catalyst is significantly greater (85 $mol_{H2O2}kg_{cat}^{-1}h^{-1}$) to that of either 0.5 wt.%Cu/CsPW (0 $mol_{H2O2}kg_{cat}^{-1}h^{-1}$) or 0.5 wt.%Pd-0.5 wt.%Cu/CsPW (4 $mol_{H2O2}kg_{cat}^{-1}h^{-1}$) despite all three catalysts having similar textural properties; namely surface area and total acidity. This is in keeping with our previous studies into the effect of Cu addition to 2.5 wt.%Au-2.5 wt.%Pd/TiO_2, with catalytic activity towards both H_2O_2 synthesis and degradation decreasing significantly with Cu incorporation, with H_2O_2 synthesis rate decreasing from 83 to 11 $mol_{H2O2}kg_{cat}^{-1}h^{-1}$ (more than 85 %) with the

addition of Cu [44]. Possibly indicating that the presence of Cu results in the blocking of active sites responsible for H_2 activation to H_2O_2. Indeed this is in agreement with previous computational studies by Joshi et al. who have determined through extensive DFT calculations that the formation of the intermediate hydroperoxy (OOH*) species, formed through the addition of hydrogen to molecular O_2, is thermodynamically unfavourable and as such H_2O_2 production is inhibited over Cu-containing supported catalysts [45].

The MgO based catalysts: 0.5 wt.%Cu/MgO, 0.5 wt.%Pd/MgO, and 0.5 wt.%Pd-0.5 wt.%Cu/MgO showed very low catalytic activity towards H_2O_2 production, with the incorporation of Cu to a 0.5 wt.%Pd/MgO catalyst leading to a complete deactivation of catalytic activity towards H_2O_2 synthesis. In contrast, these catalysts displayed the greatest activity for H_2O_2 degradation, with a significant proportion of this activity attributed to the support, which has previously been demonstrated to be highly active towards H_2O_2 degradation [30].

CONCLUSION

Pd-only, Cu-only and Cu-Pd catalysts supported on Cs-exchanged tungstophosphoric acid and MgO have been investigated for the direct synthesis of H_2O_2 from molecular hydrogen and oxygen. The heteropolyacid-based Pd catalyst is observed to be far more effective for H_2O_2 formation than the corresponding Cu-only and Cu-Pd catalysts prepared using an analogous procedure. Comparison of Pd-catalysts supported on oxides including MgO, TiO_2 and Al_2O_3 revealed that comparable H_2O_2 synthesis activity could be achieved when utilizing Cs-exchanged tungstophosphoric acid as the support despite having significantly lower Pd content, with this attributed in part to the acidic nature of the support. Moreover, we have been able to confirm computational studies that had previously suggested that the formation of H_2O_2 may be inhibited by the presence of Cu through preventing the formation of hydroperoxy species, which is a key intermediate in the production of H_2O_2.

ACKNOWLEDGEMENT

The authors would like to thank KACST for funding of this project. In addition, we thank our colleagues from Cardiff University who provided insight and expertise that greatly assisted in completing the work.

REFERENCES

1. Yu J, Shao D, Sun C, Xu C, Hinks D, (2017), *Cellulose*, **24**, 2647-2655.
2. Yu D, Wu M, Lin F, (2017), *Fibers Polym.*, **18**, 1741-1748.
3. Hage R, Lienke A, (2006), *Angew. Chem. Int. Ed.*, **45**, 206-222.
4. Babuponnusami A, Muthukuma K, (2014), *J. Environ. Chem. Eng.*, **2**, 557-572.
5. Mohammadi S, Kargari A, Sanaeepur H, Abbassian K, Najafi A, Mofarrah E, (2015), *Desalin. Water Treat.*, **53**, 2215-2234.
6. Signorile M, Crocellà V, Damin A, Rossi B, Lamberti C, Bonino F, Bordiga S, (2018), *J. Phys. Chem.C*, **122**, 9021-9034.
7. Campos-Martin JM, Blanco-Brieva G, Fierro JLG (2006) *Angew.Chem. Int. Ed.*, **45**, 6962-6984.
8. Lin M, Xia C, Zhu B, Li H, Shu X, (2016), *Chem. Eng. J.*, **295**, 370-375.
9. Seo MG, Kim HJ, Han SS, Lee KY, (2017) *Catal. Surv. Asia*, **21**, 1-12.
10. H. J. Riedl, G. Pfleiderer, I. G. Farbenindustrie AG, **1939**
11. Samanta C, Choudhary VR, (2007), *Catal. Commun.*, **8**, 73-79.
12. Choudhary VR, Samanta C, Jana P, (2007) *Appl. Catal. A*, **317**, 234-243.
13. Liu Q, Gath KK, Bauer JC, Schaak RE, Lunsford JH (2009), *Catal. Lett.*, **132**, 342-348.

14. Landon P, Collier PJ, Papworth AJ, Kiely CJ, Hutchings GJ, (2002) *Chem. Commun.*, **0**, 2058-2059.
15. Edwards JK, Thomas A, Solsona BE, Landon P, Carley AF, Hutchings GJ, (2007) *Catal. Today*, **122**, 397-402.
16. Potemkin DI, Maslov DK, Loponov K, Snytnikov PV, Shubin YV, Plyusnin PE, Svintsitskiy DA, Sobyanin VA, Lapkin AA, (2018) *Front. Chem.***6,** 85. (doi: 10.3389/fchem.2018.00085)
17. Liu Q, Bauer JC, Schaak RE, Lunsford JH, (2008), *Appl. Catal., A,* **339**, 130-136.
18. Sterchele S, Biasi P, Centomo P, Canton P, Campestrini S, Salmi T, Zecca M, (2013) *Appl. Catal., A,* **468**, 160-174.
19. Ntainjua, EN, Freakley SJ, Hutchings GJ, (2012), *Top.Catal.*, **55**, 718-722.
20. T. Deguchi, H. Yamano, S. Takenouchi and M. Iwamoto, *Catal. Sci.Technol.*, 8, 1002-1015.
21. Khan Z, Dummer NF, Edwards JK, Phil. Trans. R. Soc. A. (2018) **376**, 20170058. (doi:10.1098/rsta.2017.0058).
22. Gu J, Wang S, He Z, Han Y, Zhang J, (2016) *Catal. Sci.Tech.*, **6**, 809-817.
23. Freakley SJ, He Q, Harrhy JH, Lu L, Crole DA, Morgan DJ, Ntainjua EN, Edwards JK, Carley AF, Borisevich AY, Kiely CJ, Hutchings GJ, (2016) *Science*, **351**, 965-968.
24. Li F, Shao Q, Hu M, Chen Y, Huang X, (2018) *ACS Catal.*, **8**, 3418-3423.
25. J. Zhang, Q. Shao, Y. Zhang, S. Bai, Y. Feng and X. Huang, *Small*, 2018, **14**, 1703990. (https://doi.org/10.1002/smll.201703990)
26. Wang S, Gao K, Li W, Zhang J, (2017) *Appl.Catal. A.*, **531**, 89-95.
27. Maity S, Eswaramoorthy M, (2016) *J. Mater. Chem.*, **4**, 3233-3237.
28. Tian P, Xu X, Ao C, Ding D, Li W, Si R, Tu W, Xu J, Han YF, (2017) *ChemSusChem*, **10**, 3342-3346.
29. Xu H, Cheng D, Gao Y, (2017) *ACS Catal.*, **7**, 2164-2170.
30. Ntainjua EN, Edwards JK, Carley AF, Lopez-Sanchez JA, Moulijn JA, Herzing AA, Kiely CJ Hutchings GJ, (2008) *Green Chem.*, **10**, 1162-1169.
31. Park S, Choi JH, Kim TJ, Chung YM, Oh SH, Song IK, (2012) *Catal. Today*, **185**, 162-167.
32. Park S, Choi JH, Kim TJ, Chung YM, Oh SH, Song IK (2012) *J. Mol. Catal. A: Chem.,* **353-354**, 37-43.
33. Lewis RJ, Edwards JK, Freakley SJ, Hutchings GJ, (2017) *Ind. Eng. Chem. Res.*, **56**, 13287-13293.
34. Mori K, Furubayashi K, Okada S, Yamashita H, (2012) *RSC Adv.*, **2**, 1047.
35. Lee JW, Kim JK, Kang TH, Lee EJ, Song IK, (2017) *Catal. Today*, **293-294**, 49-55.
36. Park S, Park DR, Choi JH, Kim TJ, Chung YM, Oh SH, Song IK, *J. Mol. Catal. A: Chem*, 2011, **336**, 78-86.
37. Park S,Kim TJ, Chung YM, Oh SH, Song IK, (2010) *Res. Chem. Intermed.*, **36**, 639-646.
38. Sun M, Zhang J, Zhang Q,Wang Y, Wan H, (2009) *Chem Commun (Cambridge U.K)*, **0**, 5174-5176.
39. Ntainjua EN, Piccinini M, Freakley SJ, Pritchard JC, Edwards JK, Carley AF, Hutchings GJ, (2012) *Green Chem.* **14**, 170-181.
40. Freakley SJ, Lewis RJ, Morgan DJ, Edwards JK, Hutchings GJ, (2015) *Catalysis Today*, **248**, 10-17.
41. Park S, Lee S, Song S, Park D, Baeck S, Kim T, Chung Y, Oh S, Song I, (2009) *Catal. Commun.*, **10**, 391-394.
42. N. Essayem, Holmqvist A., Gayraud P.Y, Verdrine J.C, Taarit Y.B, (2001) *J. Catal.*, **197**, 273-280.
43. Edwards JK, Pritchard JC, Lu L, Piccinini M, Shaw G, Carley AF, Morgan DJ., Kiely CJ, Hutchings GJ., (2014) *Angew. Chem. Int. Ed*, **53**, 2381–2384.
44. Ab Rahim MH, Armstrong RD, Hammond C, Dimitratos N, Freakley SJ, Forde MM, Morgan DJ, Lalev G, Jenkins RL, Lopez-Sanchez JA, Taylor SH, Hutchings GJ, (2016) *Catal. Sci. Technol.*, **6**, 3410-3418.
45. Joshi AM, Delgass WN, Thomson KT, (2007) *J. Phys. Chem. C.*, **111**, 7384-7395.